

# Effect of dental implant macrogeometry on the probability of survival and strain distribution of an implant–abutment set

Monalisa Barbosa Pereira<sup>1,B</sup>, Livia Fiorin<sup>1,B,D</sup>, Adriana Cláudia Lapria Faria<sup>1,C–F</sup>, Estevam Augusto Bonfante<sup>2,C,E</sup>, Ricardo Faria Ribeiro<sup>1,A,C,E,F</sup>, Renata Cristina Silveira Rodrigues<sup>1,A,C,E,F</sup>

<sup>1</sup> Department of Dental Materials and Prosthodontics, Ribeirão Preto School of Dentistry, University of São Paulo, Ribeirão Preto, Brazil

<sup>2</sup> Department of Prosthodontics and Periodontics, Bauru School of Dentistry, University of São Paulo, Bauru, Brazil

A – research concept and design; B – collection and/or assembly of data; C – data analysis and interpretation;

D – writing the article; E – critical revision of the article; F – final approval of the article

Dental and Medical Problems, ISSN 1644-387X (print), ISSN 2300-9020 (online)

*Dent Med Probl.* 2025;62(3):537–545

## Address for correspondence

Ricardo Faria Ribeiro  
E-mail: rribeiro@usp.br

## Funding sources

The study was funded by the Coordination for the Improvement of Higher Education Personnel (CAPES), the São Paulo Research Foundation (FAPESP) (grant No. 2021/06730-7), and the National Council for Scientific and Technological Development (CNPq) (grant No. 307255/2021-2).

## Conflict of interest

None declared

## Acknowledgements

The authors would like to thank the Coordination for the Improvement of Higher Education Personnel (CAPES) for a scholarship grant and the support of the Oral Rehabilitation Graduate Program, as well as the São Paulo Research Foundation (FAPESP) and the National Council for Scientific and Technological Development (CNPq) for scholarship grants.

Received on August 29, 2023

Reviewed on October 13, 2023

Accepted on October 18, 2023

Published online on June 30, 2025

## Cite as

Pereira MB, Fiorin L, Faria ACL, Bonfante EA, Ribeiro RF, Rodrigues RCS. Effect of dental implant macrogeometry on the probability of survival and strain distribution of an implant–abutment set. *Dent Med Probl.* 2025;62(3):537–545. doi:10.17219/dmp/174298

## DOI

10.17219/dmp/174298

## Copyright

Copyright by Author(s)

This is an article distributed under the terms of the

Creative Commons Attribution 3.0 Unported License (CC BY 3.0)

(<https://creativecommons.org/licenses/by/3.0/>).

## Abstract

**Background.** The effect of the macrogeometry of dental implants with double trapezoidal threads on the probability of survival and the long-term success of oral rehabilitation is unclear.

**Objectives.** The purpose of this in vitro study was to evaluate the effect of dental implant macrogeometry on the probability of survival, failure mode and strain distribution of an implant–abutment set.

**Material and methods.** Dental implants were divided into 2 groups according to their macrogeometry ( $n = 21$  per group): trapezoidal thread (control group); and double trapezoidal thread (test group). The macrogeometry analysis was performed with the use of computed microtomography ( $n = 1$ ). The specimens were subjected to single load to failure (SLF) ( $n = 3$ ), which permitted the step-stress profiles for design-based step-stress accelerated life testing (SSALT) ( $n = 18$ ). The probability of survival and reliability for a mission of 50,000 cycles were calculated at 100 N and 150 N. The scanning electron microscope (SEM) was used to analyze the failure mode of the implant–abutment set. The digital image correlation (DIC) ( $n = 3$ ) was performed using the implant–abutment set embedded in a polyurethane resin subjected to a static load of 250 N in axial and non-axial positions.

**Results.** No statistically significant differences were observed between the groups with respect to the probability of survival. All groups showed a reliability level higher than 95% at 100 N, while a decrease in reliability was observed at 150 N. The Weibull modulus and characteristic resistance exhibited no significant differences between the groups. The  $\beta$  mean values (control = 0.66, test = 0.33) indicated that failures were dictated by material strength. The SEM revealed an abutment and implant body fracture, characterized by fracture initiation on the lingual surface that subsequently propagated to the opposing buccal side. In the context of non-axial loading, the test group exhibited a higher concentration of tensile strain in the cervical region (152.05  $\mu\text{s}$ ), while the control group exhibited a predominance of compression strain (–800.00  $\mu\text{s}$ ).

**Conclusions.** The macrogeometry of dental implants did not influence the failure mode and probability of survival, but modified the strain distribution of the implant–abutment set.

**Keywords:** dental implants, macrogeometry, probability of survival, strain distribution

## Highlights

- The macrogeometry of dental implants, including parallel and double trapezoidal threads, did not affect the failure mode or survival probability under clinically relevant loads for anterior teeth.
- Both implant designs exhibited high reliability (95–98%) at 100 N, but reliability decreased at higher loads (150 N).
- Double trapezoidal threads caused higher tensile strain in the cervical region under non-axial loading, potentially increasing fracture risk in the implant–abutment assembly.

## Introduction

The predictability and long-term success rate of dental implant treatment have been related to several factors, including material biocompatibility, management of surgical technique, bone quality, loading conditions, surface treatments, and implant geometry.<sup>1,2</sup> Implant geometry refers to the three-dimensional implant structure, and may be categorized into 2 modalities, namely macrogeometry and microgeometry. Macrogeometry refers to the prosthetic connection, implant body and thread design, while microgeometry is related to the surface treatment, surface morphology and implant material.<sup>3,4</sup> The macrogeometry of dental implants comprises factors such as implant diameter, length, surface characteristics, and thread design.

New dental implant macrogeometries, which include models with deep threads and a smaller thread pitch, were developed to increase primary implant stability and improve strain distribution to the peri-implant bone, especially in cases of low bone quality (III and IV bone type), implant placement after extraction, and immediate loading protocols.<sup>3–5</sup> The macrogeometry of implants is related to the longevity of treatment, because it determines bone-to-implant contact, masticatory strain distribution and the mechanical strength of the implant.<sup>3–5</sup>

Mechanical complications are frequent in implant dentistry. Preclinical studies can simulate the conditions present in the oral environment and predict clinical performance. One of the mechanical complications is implant fracture. An inadequate implant diameter and length, especially in cases of compromised bone quality or high occlusal forces, can increase the risk of implant fracture, compromising the overall implant stability and longevity. Additionally, the lack of a suitable thread design and surface characteristics can further exacerbate this risk. Another complication associated with macrogeometry is screw loosening. An insufficient implant diameter, thread pitch or inadequate surface roughness can result in ineffective retention of the abutment screw. This can lead to improper load distribution, compromised esthetics and implant failure over time.<sup>6–10</sup> While static testing can be helpful in ranking different implant systems' load to failure performance, structural failure is

time-dependent as a function of the implant–abutment set. Higher complication rates have been observed with longer usage times. Therefore, the fatigue test is considered a clinically relevant predictor of material strength.<sup>11</sup> Some authors have evaluated the influence of macrogeometry on the fatigue behavior of dental implants,<sup>12–18</sup> and most of them found that the diameter of the implant influences the fatigue behavior,<sup>14–16</sup> whereas the influence of the characteristics of the implant thread on the fatigue behavior of the implant–abutment set is uncertain.<sup>19</sup>

Digital image correlation (DIC) is a non-contact optical method used to evaluate the strain distribution on the surface of a material during a mechanical test. To that end, several images are captured using a camera and analyzed by specialized software, which calculates the displacement of the surface points.<sup>20,21</sup> A number of studies have compared the results of DIC with those of photoelasticity<sup>22</sup> and finite element analysis (FEA).<sup>23,24</sup> The authors found that the distribution of surface deformation is comparable, thereby validating the model and visualizing the strain distribution of dental implants and implant-supported prostheses.<sup>22–28</sup> Therefore, the purpose of this study was to evaluate the failure mode and probability of survival of the implant–abutment set, composed of dental implants with internal conical connection and different microgeometries. These implants were subjected to step-stress accelerated life testing (SSALT) and strain distribution using DIC. The null hypothesis stated that the macrogeometry of dental implants with internal conical connection does not influence the failure mode, probability of survival and strain distribution of the implant–abutment set.

## Material and methods

Titanium dental implants with a conical shape and internal conical connection were divided into 2 groups ( $n = 21$  per group), according to their macrogeometry: a control group, represented by implants with trapezoidal threads (CM implants; Singular Implants, Parnamirim, Brazil); and a test group, represented by implants with double trapezoidal threads (Go Direct CM; Singular Implants) (Fig. 1, Table 1).

**Table 1.** Characteristics of dental implants used in the study

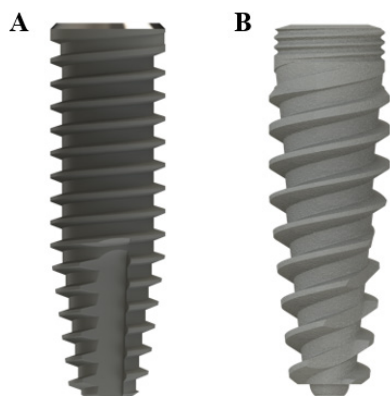
Characteristic	Control group	Test group
Commercial name	CM implants (Singular Implants, Parnamirim, Brazil)	Cone Morse Go Direct (Singular Implants, Parnamirim, Brazil)
Diameter [mm]	3.5	3.5
Length [mm]	11.5	11.5
Indication	III and IV bone types	I, II, III, and IV bone types
Cervical zone	presents at 0.4 mm between the platform and the threads	presents at 1.0 mm with pyramidal microthreads, improving secondary stability and preventing bone loss
Body	cylindrical with a conical apex	the body diameter is larger than the platform diameter, and it has a conical apex with a 0.6-mm chamfer
Active apex	soft, rounded, small tip and 3 flutes	soft, rounded, small tip and 1 helicoidal flute
External threads	trapezoidal	double trapezoidal
Thread pitch [mm]	0.80	1.00
Thread depth [mm]	0.40	0.40–0.55

The probability of survival was determined using SSALT.<sup>14,15,17–19,25</sup> The implants were positioned in a 30° inclination matrix according to ISO 14801:2016, and embedded in a polyurethane resin with the implant platform positioned 3 mm above the resin level, simulating 3 mm of bone resorption. The prefabricated universal abutments (Singular Implants) were then connected to the implants, tightened using a digital torque gauge (TQ-680; Instrutherm, São Paulo, Brazil) (32 N·cm), and covered with a stainless steel hemispherical loading member. Three specimens from each group were subjected to single load to fracture (SLF) in a universal testing machine (Biopdi, São Paulo, Brazil), with a 1000-kgf load cell and a displacement of 1 mm/min. Three loading profiles were designed for SSALT ( $n = 18$ ) (Fig. 2) and labeled as light ( $n = 9$ ), moderate ( $n = 6$ ) or aggressive ( $n = 3$ ), according to the ratio distribution of 3:2:1.<sup>11,15,17–19,25</sup> The force used in each loading profile ranged between 20% and 60% of the SLF mean value.<sup>11</sup> Step-stress accelerated life testing was performed using a fatigue test equipment (Biopdi), with

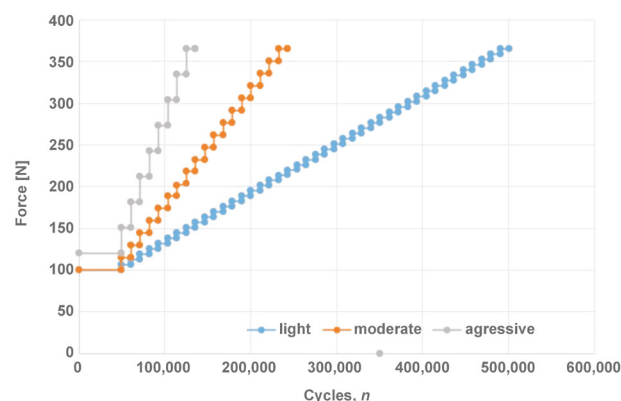
an isometric loading protocol, 4 Hz, in water at 37°C (Fig. 3). The specimens were cycled until failure or until reaching the loading limit. At the end of each cycle, they were analyzed to verify the presence of any deformations and/or fractures.

The failure mode analysis ( $n = 3$ ) was performed qualitatively using a scanning electron microscope (SEM) (EVO MA10; Zeiss, Oberkochen, Germany) under  $\times 90$  and  $\times 500$  magnification to identify the origin and direction of crack propagation.

A qualitative analysis was conducted by means of computed microtomography ( $n = 1$ ) (SkyScan 1176; Bruker, Kontich, Belgium) using the following scanning parameters: 90 kV; 272 mA; a copper (Cu) filter with an exposure time of 81 ms per image in 360°; 9- $\mu$ m isotropic voxel; and a frame of 4. The images were obtained before SSALT and reconstructed using the NRecon v.1.6.9.18 software (Bruker). The image of the implant with the best quality was selected. The analysis of implant macrogeometry (wall thickness, depth and thread pitch) was performed using the linear measurement tool of the CTan software, v.1.14.4.1+ (Bruker).

**Fig. 1.** Dental implants evaluated in the study

A. Implant with a trapezoidal thread (control group); B. Implant with a double trapezoidal thread (test group).

**Fig. 2.** Graphic representation of loading profiles designed for step-stress accelerated life testing (SSALT)

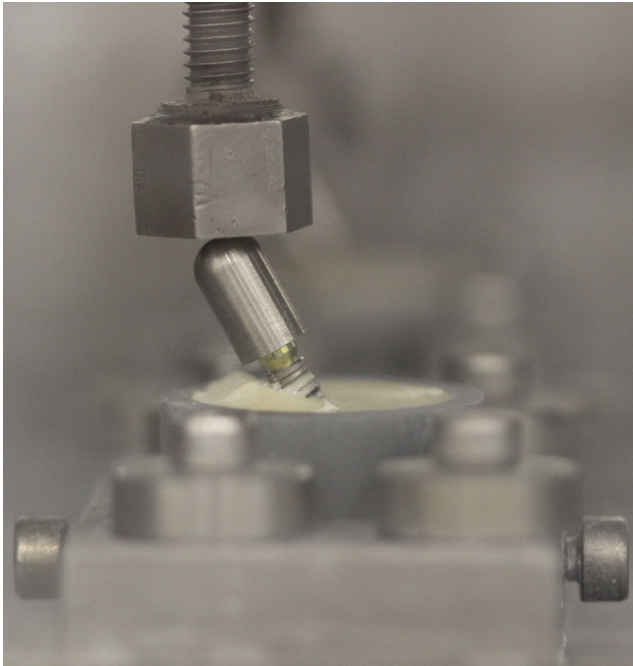


Fig. 3. Implant–abutment hemispherical loading member positioned for SSALT

The distribution of strain around the implant was analyzed using DIC ( $n = 3$ ).<sup>21–24,26–28</sup> The master model of polymethylmethacrylate (PMMA) was made with dimensions of 55 mm × 30 mm × 14 mm (length, height and depth, respectively), and the implant–abutment set was fixed with cyanoacrylate glue (Super Bonder; Loctite, São Paulo, Brazil). After 24 h, an impression of the PMMA master model was obtained using silicone (Silikon; Odontomega, Ribeirão Preto, Brazil). The implant–abutment set was embedded in polyurethane resin (F16; Axson Technologies, Cergy, France), thereby capturing the predefined position of the implant. The surface of each model was coated with a thin layer of white paint (Colorgin Premium; Colorgin, Taboão da Serra, Brazil) and with small black spray dots (Colorgin) (Fig. 4).<sup>22,26,27</sup> A random surface pattern was applied to all models with speckles simultaneously, and it was calibrated using a plate with black dots provided by the manufacturer.

The digital image correlation complete system (StrainMaster; Polytec GmbH, Waldbronn, Germany) included 2 charge-coupled device (CCD) digital cameras (Imager E-lite 2M, 1101132; LaVision GmbH, Göttingen, Germany), with a resolution of 1,039 × 1,395 pixels, which were used to capture images of the model under loading. The DaVis 8.0 software (LaVision GmbH) was employed for image analysis and strain calculation. Two types of load application were used: axial (model positioned horizontally); and non-axial (model positioned on an acrylic base with an angle of 30°). Static loads were applied using a universal testing machine (Biopdi) with a load cell of 50 kgf, a test speed of 1 mm/min, and up to a load of 250 N.<sup>22,26,27</sup> During load application, point dislodgement was tracked by the software in order to calculate the strain on the model surface. The qualitative

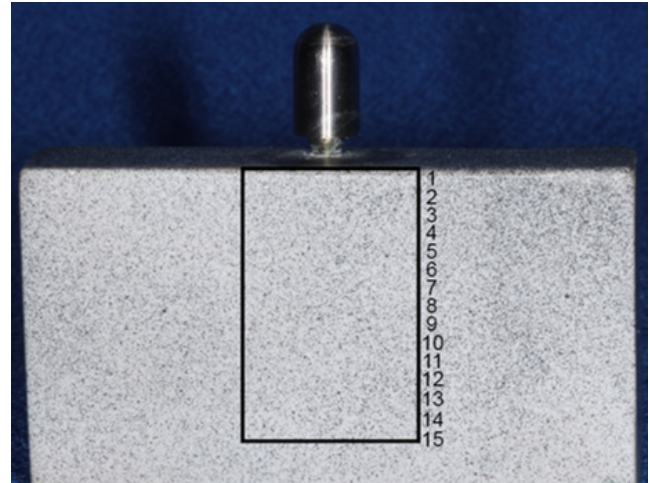


Fig. 4. Polyurethane model with small black dots showing the region analyzed using digital image correlation (DIC) with vertical distance measurement along the implant

analysis of the images was based on a color scale, with positive values (ranging from yellow to red) denoting tensile strain and negative values (ranging from green to blue) indicating compressive strain. To ensure the repeatability and reliability of the DIC, 3 loadings were performed on each model, and the results were analyzed.

## Statistical analysis

For SSALT, the use level probability Weibull curve (probability of failure vs. the number of cycles) was calculated (Alta Pro 9; ReliaSoft, Tucson, USA) using as a parameter 60% of the maximum load found in SLF and a bilateral 90% confidence interval (*CI*). The reliability was calculated for a mission of 50,000 cycles at 100 N and 150 N, and the differences between these missions were identified through the implementation of the Weibull calculation with a two-way 90% *CI*.

## Results

The mean values obtained in SLF were 539.86 N for the control group and 676.12 N for the test group. The mean of the 2 groups (607.99 N) was used to establish the applied load on the SSALT light, moderate and aggressive loading profiles. The  $\beta$  mean values derived from the use level probability Weibull plot (two-way 90% *CI*) were 0.66 and 0.33 for the control and test groups, respectively. These findings indicate that failures were dictated by material strength, which is associated with premature failures and not with fatigue damage accumulation. The results of the Weibull distribution (Weibull modulus ( $m$ ) and characteristic resistance ( $\eta$ )) demonstrated no differences between the groups, considering the overlap of *CI*s (Fig. 5).

The reliability of the mission (50,000 cycles) at 100 N and 150 N showed no significant differences between the groups (Table 2). The probability of survival decreased for



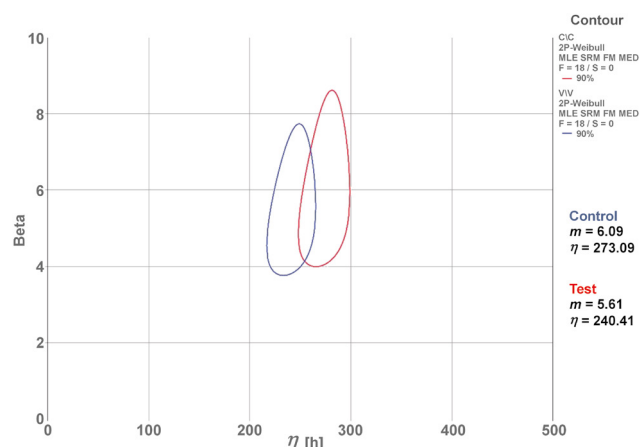


Fig. 5. Weibull contour plot

MLE – maximum likelihood estimation; SRM – standard regression method; FM – Fisher matrix; MED – median ranks; F – probability of failure; S – probability of survival; C/C – control group; V/V – test group.

both groups at 150 N, indicating that cumulative damage at higher loadings is associated with lower survival, especially in the test group (57%).

Table 2. Reliability calculated for a mission of 50,000 cycles according to the applied load

Variable	Control group		Test group	
	100 N	150 N	100 N	150 N
Upper limit	1.00	0.90	0.98	0.71
Reliability	0.98	0.79	0.95	0.57
Lower limit	0.92	0.59	0.87	0.39
$\beta$	0.66		0.33	

All specimens failed after SSALT, and the failure was restricted to fractures in the abutment and implant, specifically between the region of the third thread of the implant and the first thread of the abutment. The SEM micrographs demonstrated the failure mode of fractured specimens. The fracture's initiation was attributed to tensile strain on the lingual surface, with propagation to the buccal surface. A representative image of the SEM revealed the fracture origin, crack propagation direction (Fig. 6A,B) and the presence of longitudinal cracks on the internal walls of the hexagon vertex (Fig. 6C,D).

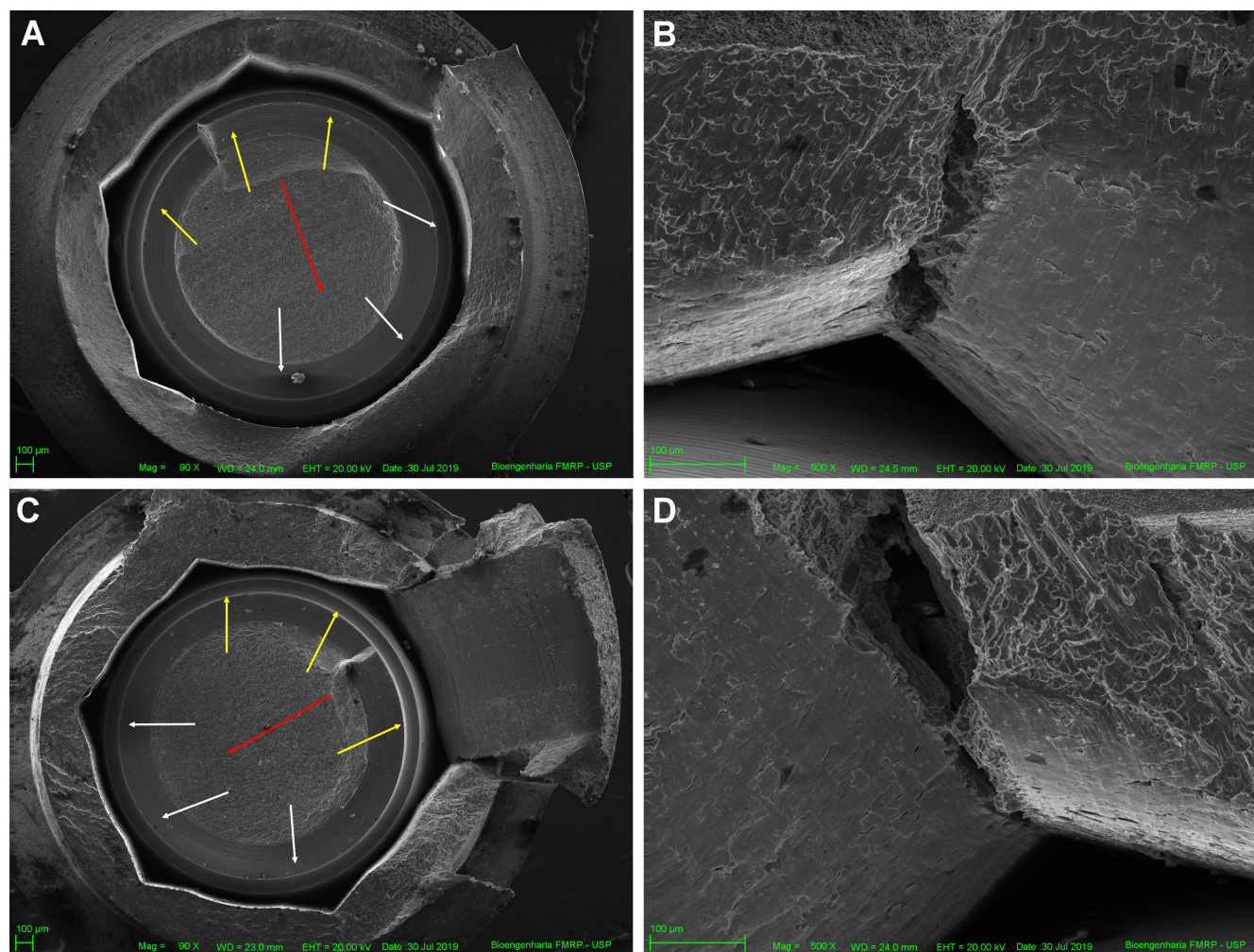


Fig. 6. Scanning electron micrographs of the fractured implant–abutment set after SSALT

A,B. Control group; C,D. Test group; WD – working distance; EHT – extra high tension. The yellow arrows denote the fracture origin, the red arrows indicate the direction of crack propagation, and the white arrows represent compressive strain.



The two-dimensional qualitative analysis with computed microtomography revealed differences in the macrogeometry of the groups, including thread pitch (control = 0.805 mm, test = 1.696 mm), thread depth (control = 0.381 mm, test = 0.402 mm) and wall thickness (control = 0.294 mm, test = 0.304 mm). Furthermore, a difference was observed in the cross-section of the 2 implants (control – trapezoidal, test – double trapezoidal).

The strain generated under axial and non-axial loading is illustrated in Fig. 7 and 8, respectively. The qualitative analysis of DIC showed a predominance of tensile strain in the middle and apical regions, and compressive strain in the cervical zone in both groups exposed to axial loading. The application of non-axial loading resulted in strain concentration in the middle and apical regions of the control group, and a substantial tensile strain concentration

in the cervical zone of the test group. Figure 9 presents the distribution of strain generated along the implant. All groups showed similar behavior under axial loading. In non-axial loading, the control group demonstrated a strain distribution that was analogous to that observed in axial loading. Conversely, the test group exhibited a predominance of tensile strain concentration, especially in the cervical zone.

## Discussion

The knowledge about the effect of dental implant macrogeometry on the fatigue behavior of the implant–abutment set is important due to its potential to predict clinical complications.<sup>5,11</sup> Therefore, this study evaluated

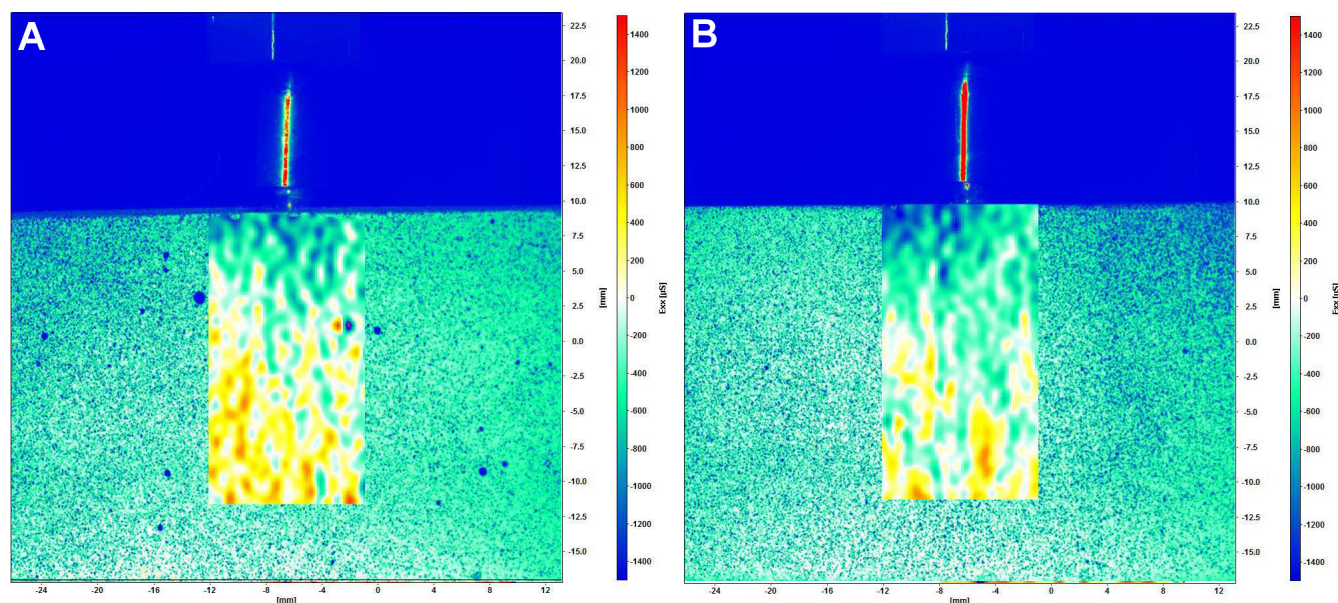


Fig. 7. Surface strain under axial loading at 250 N  
A. Control group; B. Test group.

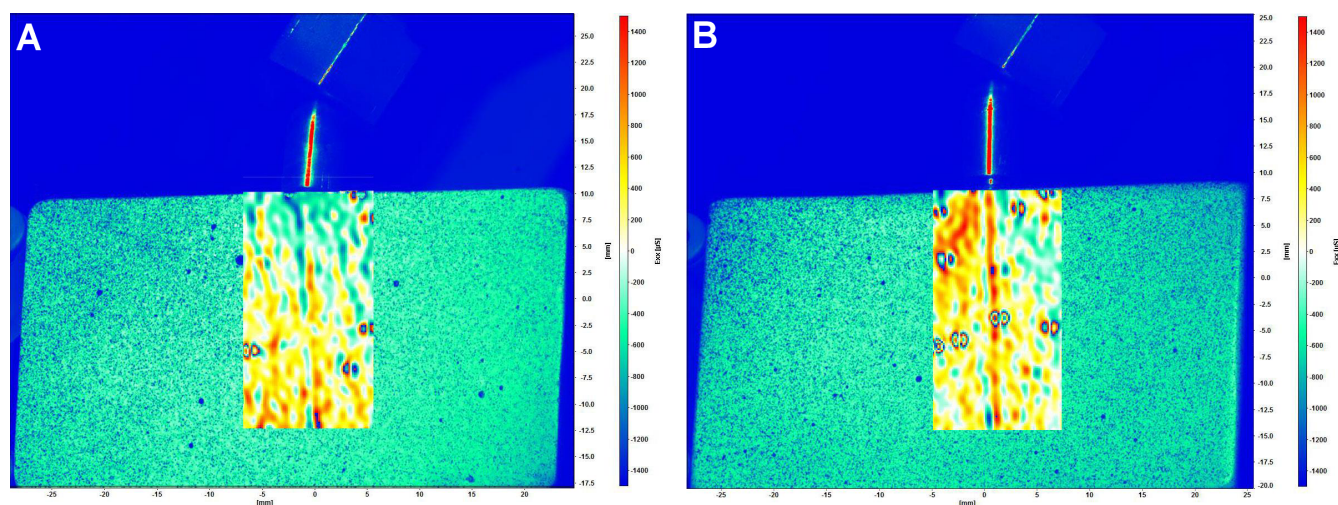


Fig. 8. Surface strain under non-axial loading at 250 N  
A. Control group; B. Test group.

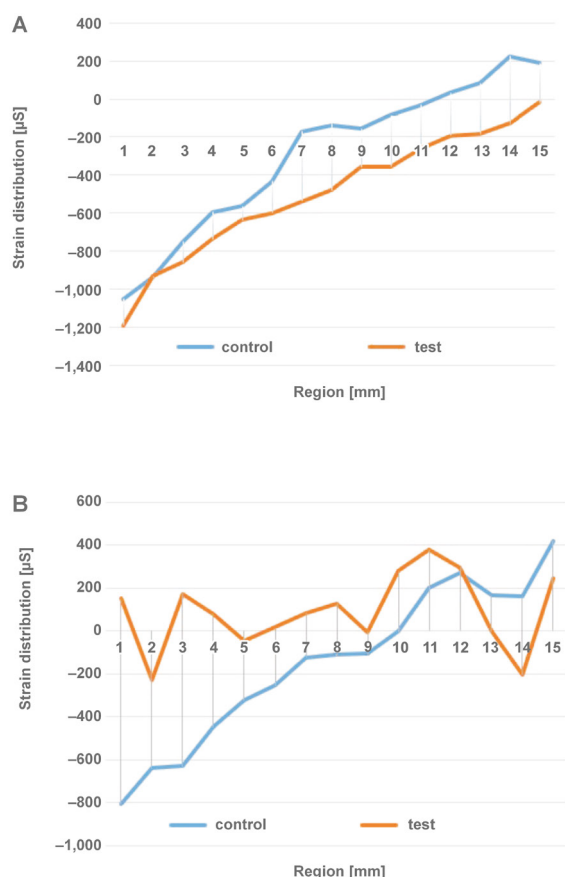


Fig. 9. Strain distribution around the implant after axial (A) and non-axial loading (B)

The horizontal axis represents the vertical distance measurements along the implant, as presented in Fig. 4.

the failure mode and probability of survival of dental implants with internal conical connection and different macrogeometries, including differences in the shape, pitch and depth of threads. The null hypothesis was partially accepted. The implant macrogeometry had no influence on the failure mode or probability of survival; however, there was a difference in stress transmission between the groups.

The specimens were subjected to cyclic loading during SSALT. The load levels increased successively until failure or suspension to reproduce the failure modes found clinically.<sup>11</sup> The results suggest that all implant macrogeometries presented high reliability (95–98%), simulating maximum bite forces found in the anterior region (100 N). Thus, they can be considered a reliable option for incisors.<sup>29,30</sup> In the posterior regions, the load-bearing capacity ranged between 300 N and 800 N.<sup>31</sup> However, the results of the present study should only be compared to the load-bearing capacity found in the anterior regions due to the positioning of the specimens at a 30° angle and the 3-mm exposure of the implant in the cervical region. This configuration simulates a worst-case scenario. On the other hand, loading in posterior crowns occurs in axial loading. A non-significant reduction in reliability was observed in both groups at 150 N. Bordin et al. found

a similar probability of survival for narrow and extra-narrow dental implants with internal conical connection subjected to SSALT.<sup>17</sup> Both groups demonstrated high reliability at 50 N and 100 N, and there was a decrease in reliability at 150 N and 180 N, though no significant differences were observed between the groups.

The  $\beta$  value revealed by the SSALT data analysis is essential to understand the lifetime failure rate.<sup>11,19</sup> Both groups showed  $\beta$  value  $<1$ , indicating that failures of the implant–abutment set were dictated by the strength of the material, which is associated with premature failures. Failures attributable to the strength of the material were also reported by other authors.<sup>12,17–19</sup> Although the control group exhibited higher values of characteristic resistance and Weibull modulus than the test group, a statistical difference between the 2 groups was not identified. The Weibull modulus was used as an indicator of survival force and force distribution, predicting the presence of flaws in the material structure. The higher values observed in the control group indicated homogeneous failure distribution, low data dispersion, structural stability, and greater reliability.<sup>11,32,33</sup>

Previous studies have reported various failure modes of the implant–abutment set after SSALT, such as screw abutment fracture, abutment fracture,<sup>12,13,15,17–19</sup> and fracture of the implant body.<sup>17</sup> In the current study, the most prevalent failure mode was abutment fracture and implant body fracture, particularly in the region between the third thread of the implant and the first thread of the abutment. Scanning electron micrographs revealed fatigue and overload areas, corroborating the results of Weibull analysis, which stated that failures were caused by the strength of the material. The fracture originated when the strain exceeded the titanium strength, creating the deformation process and the formation of a plastic zone. This ultimately resulted in the fracture of the ductile implant body.<sup>18</sup>

In the present study, DIC illustrated tensile strain distribution under axial and non-axial loading conditions. Non-axial loading was performed using the same angulation as the specimens that were subjected to SSALT. The digital image correlation was used to analyze the surface strain of simulated bone models under a static load. This method offers the advantage of being easy to implement without disturbing the specimen, regardless of its type and size,<sup>34,35</sup> and to allow the precise full-field strain measurement. The DIC method offers the clear advantage of using real parts, which are very similar or even identical to those manufactured for patients in the clinic. This method ensures accuracy and repeatability, thereby facilitating analysis. Several studies<sup>16–19,21–23</sup> have indicated that DIC, despite manifesting tensions on the surface of models, corresponded accurately to findings derived from alternative test methods, such as finite element analysis.<sup>30</sup> Furthermore, these methodologies are not in competition with one another; rather, they are regarded as complementary approaches, allowing for a more profound



observation of the phenomena under study and facilitating the formulation of more substantiated conclusions. This, in turn, paves the way for novel studies aimed at advancing the knowledge available to clinicians.

Previous studies<sup>21,34,35</sup> have found that axial loading resulted in a better mechanical response, whereas non-axial loading exhibited the highest strain concentration in the cervical region of a dental implant.<sup>21</sup> The present study found high concentration of tensile strain in the cervical region of the implant in both groups, which contributed to abutment and implant body fracture. The test group exhibited a higher concentration of strain in the cervical region, demonstrating that dental implants with double trapezoidal threads presented a higher strain concentration in this region than implants with parallel threads. Accordingly, Freitas et al. evaluated the probability of survival and strain distribution of implants with internal conical connection and different microgeometries.<sup>19</sup> The researchers noted that dental implants with double trapezoidal threads presented a higher strain concentration in the implant and cortical bone.<sup>19</sup>

The present study demonstrated that the macrogeometry of dental implants had no effect on the probability of survival; however, it modified the strain distribution of the implant–abutment set. Dental implants with parallel and double trapezoidal threads presented comparable strain distribution during axial loading, but double trapezoidal threads resulted in a higher tensile strain concentration in the cervical region during non-axial loading than parallel ones. A limitation of this study is the construction of a crown, which was not modeled with the materials usually chosen in clinical settings. Thus, considering that materials used in the fabrication of abutments and crowns (metal alloys, zirconia, polyether ether ketone) can influence the distribution of deformations within the implant–abutment–crown assembly<sup>26,36</sup> due to shock absorption or not,<sup>36</sup> translating these results into clinical practice necessitates meticulous consideration. It is important to acknowledge the limitations of in vitro studies and to exercise caution when interpreting their results. The limitations of this study include the absence of an anatomical crown. Step-stress accelerated life testing did not assess complex factors found in the oral cavity, such as occlusal loading dynamics, neuromuscular forces and parafunctional habits. The models used for DIC were manufactured using a polyurethane resin that was solid, homogeneous, devoid of porosity, and isotropic. Despite these limitations, the results of this in vitro study demonstrated potential causes of implant–abutment set failures, establishing the foundation for future research. Our results must be validated by clinical trials that assess the influence of macrogeometry on treatment longevity.

Mechanical complications related to the macrogeometry of dental implants pose significant challenges to the long-term success of treatment. A comprehensive analysis and planning, encompassing the implant diameter,

length, thread design, and surface characteristics, can help minimize these complications. Having achieved this objective, it is possible to guarantee optimal implant macrogeometry, enhancing implant longevity, patient satisfaction and oral health. Further research is required to develop advanced implant designs that effectively prevent these mechanical complications.

## Conclusions

The results of this in vitro study demonstrated that the tested macrogeometries of dental implants exhibited a high probability of survival at loads that are clinically relevant for anterior teeth. Failure modes were restricted to abutment and implant body fracture. A higher concentration of tensile strain was observed in the cervical region of the dental implant when double trapezoidal threads were used in comparison to parallel threads.

## Ethics approval and consent to participate

Not applicable.

## Data availability

The datasets generated and/or analyzed during the current study are available from the corresponding author on reasonable request.

## Consent for publication

Not applicable.


## Use of AI and AI-assisted technologies


Not applicable.


## ORCID iDs

Monalisa Barbosa Pereira  <https://orcid.org/0000-0002-1953-2352>


Livia Fiorin  <https://orcid.org/0000-0001-5109-4033>

Adriana Cláudia Lapria Faria  <https://orcid.org/0000-0001-6353-1480>

Estevam Augusto Bonfante  <https://orcid.org/0000-0001-6867-8350>

Ricardo Faria Ribeiro  <https://orcid.org/0000-0003-4211-0542>

Renata Cristina Silveira Rodrigues

 <https://orcid.org/0000-0003-4140-4143>

## References

1. Amid R, Raoofi S, Kadkhodazadeh M, Movahhedi MR, Khademi M. Effect of microthread design of dental implants on stress and strain patterns: A three-dimensional finite element analysis. *Biomed Tech (Berl)*. 2013;58(5):457–467. doi:10.1515/bmt-2012-0108
2. Dommeti VK, Pramanik S, Roy S. Design of customized coated dental implants using finite element analysis. *Dent Med Probl*. 2023;60(3):385–392. doi:10.17219/dmp/142447
3. Steigenga JT, Al-Shammari KF, Nociti FH, Misch CE, Wang HL. Dental implant design and its relationship to long-term implant success. *Implant Dent*. 2003;12(4):306–317. doi:10.1097/01.id.0000091140.76130.a1



4. Abuhussein H, Pagni G, Rebaudi A, Wang HL. The effect of thread pattern upon implant osseointegration. *Clin Oral Implants Res.* 2010;21(2):129–136. doi:10.1111/j.1600-0501.2009.01800.x
5. Udomsawat C, Rungsiyakull P, Rungsiyakull C, Khongkhunthian P. Comparative study of stress characteristics in surrounding bone during insertion of dental implants of three different thread designs: A three-dimensional dynamic finite element study. *Clin Exp Dent Res.* 2018;5(1):26–37. doi:10.1002/cre2.152
6. Comuzzi L, Tumedei M, De Angelis F, Lorusso F, Piatelli A, Iezzi G. Influence of the dental implant microgeometry and threads design on primary stability: An in vitro simulation on artificial bone blocks. *Comput Methods Biomech Biomed Engin.* 2021;24(11):1242–1250. doi:10.1080/10255842.2021.1875219
7. Gehrke SA, Eliers Treichel TL, Pérez-Díaz L, et al. Impact of different titanium implant thread designs on bone healing: A biomechanical and histometric study with an animal model. *J Clin Med.* 2019;8(6):777. doi:10.3390/jcm8060777
8. Pjetursson BE, Asgeirsson AG, Zwahlen M, Sailer I. Improvements in implant dentistry over the last decade: Comparison of survival and complication rates in older and newer publications. *Int J Oral Maxillofac Implants.* 2014;Suppl 29:308–324. doi:10.11607/jomi.2014suppl.g5.2
9. Larsson A, Manuh J, Chrcanovic BR. Risk factors associated with failure and technical complications of implant-supported single crowns: A retrospective study. *Medicina (Kaunas).* 2023;59(9):1603. doi:10.3390/medicina59091603
10. Jung RE, Zembic A, Pjetursson BE, Zwahlen M, Thoma DS. Systematic review of the survival rate and the incidence of biological, technical, and aesthetic complications of single crowns on implants reported in longitudinal studies with a mean follow-up of 5 years. *Clin Oral Implants Res.* 2012;23 Suppl 6:2–21. doi:10.1111/j.1600-0501.2012.02547.x
11. Bonfante EA, Coelho PG. A critical perspective on mechanical testing of implants and prostheses. *Adv Dent Res.* 2016;28(1):18–27. doi:10.1177/0022034515624445
12. Freitas-Junior AC, Bonfante EA, Martins LM, Silva NRFA, Marotta L, Coelho PG. Effect of implant diameter on reliability and failure modes of molar crowns. *Int J Prosthodont.* 2011;24(6):557–561. PMID:22146255.
13. Hirata R, Bonfante EA, Machado LS, Tovar N, Coelho PG. Mechanical evaluation of four narrow-diameter implant systems. *Int J Prosthodont.* 2014;27(4):359–362. doi:10.11607/ijp.3926
14. Shemtov-Yona K, Rittel D, Levin L, Machtei EE. Effect of dental implant diameter on fatigue performance. Part I: Mechanical behavior. *Clin Implant Dent Relat Res.* 2014;16(2):172–177. doi:10.1111/j.1708-8208.2012.00477.x
15. Freitas GP, Hirata R, Bonfante EA, Tovar N, Coelho PG. Survival probability of narrow and standard-diameter implants with different implant–abutment connection designs. *Int J Prosthodont.* 2016;29(2):179–185. doi:10.11607/ijp.4232
16. Song SY, Lee JY, Shin SW. Effect of implant diameter on fatigue strength. *Implant Dent.* 2017;26(1):59–65. doi:10.1097/ID.0000000000000502
17. Bordin D, Bergamo ETP, Fardin VP, Coelho PG, Bonfante EA. Fracture strength and probability of survival of narrow and extra-narrow dental implants after fatigue testing: In vitro and in silico analysis. *J Mech Behav Biomed Mater.* 2017;71:244–249. doi:10.1016/j.jmbbm.2017.03.022
18. Bordin D, Bergamo ETP, Bonfante EA, Fardin VP, Coelho PG. Influence of platform diameter in the reliability and failure mode of extra-short dental implants. *J Mech Behav Biomed Mater.* 2018;77:470–474. doi:10.1016/j.jmbbm.2017.09.020
19. Freitas MIM, Gomes RS, Ruggiero MM, et al. Probability of survival and stress distribution of narrow diameter implants with different implant–abutment taper angles. *J Biomed Mater Res B Appl Biomater.* 2022;110(3):638–645. doi:10.1002/jbm.b.34942
20. Li J, Fok ASL, Satterthwaite J, Watts DC. Measurement of the full-field polymerization shrinkage and depth of cure of dental composites using digital image correlation. *Dent Mater.* 2009;25(5):582–588. doi:10.1016/j.dental.2008.11.001
21. Tribst JPM, Dal Piva AMO, Bottino MA, Nishioka RS, Borges ALS, Özcan M. Digital image correlation and finite element analysis of bone strain generated by implant-retained cantilever fixed prosthesis. *Eur J Prosthodont Restor Dent.* 2020;28(1):10–17. doi:10.1922/EJPRD\_1941Tribst08
22. Tiozzi R, de Torres EM, Rodrigues RCS, et al. Comparison of the correlation of photoelasticity and digital imaging to characterize the load transfer of implant-supported restorations. *J Prosthodont.* 2014;112(2):276–284. doi:10.1016/j.prosdent.2013.09.029
23. Demachkia AM, Sichi LGB, Rodrigues JVM, et al. Implant-supported restoration with straight and angled hybrid abutments: Digital image correlation and 3D-finite element analysis. *Eur J Gen Dent.* 2022;11(1):23–31. doi:10.1055/s-0042-1744362
24. Yang B, Irastorza-Landa A, Heuberger P, Ploeg HL. Digital image correlation validation of finite element strain analysis of dental implant insertion for two implant designs. In: *Proceedings of the ASME 2023 Verification, Validation, and Uncertainty Quantification Symposium*; 2023. doi:10.1115/VVUQ2023-107659
25. Benalcázar Jalkh EB, de Souza Neto J, Bergamo ETP, Maia CF, Bonfante EA. Mechanical testing of four-unit implant-supported prostheses with extensive pink gingiva porcelain: The dentogingival prostheses proof of concept. *J Esthet Restor Dent.* 2021;33(4):605–612. doi:10.1111/jerd.12704
26. Tiozzi R, Gomes ÉA, Faria ACL, Rodrigues RCS, Ribeiro RF. Biomechanical behavior of titanium and zirconia frameworks for implant-supported full-arch fixed dental prosthesis. *Clin Implant Dent Relat Res.* 2017;19(5):860–866. doi:10.1111/cid.12525
27. Peixoto RF, Tonin BSH, Martinelli J, Macedo AP, de Mattos MGC. In vitro digital image correlation analysis of the strain transferred by screw-retained fixed partial dentures supported by short and conventional implants. *J Mech Behav Biomed Mater.* 2020;103:103556. doi:10.1016/j.jmbbm.2019.103556
28. Yoon S, Jung HJ, Knowles JC, Lee HH. Digital image correlation in dental materials and related research: A review. *Dent Mater.* 2021;37(5):758–771. doi:10.1016/j.dental.2021.02.024
29. Fontijn-Tekamp FA, Slagter AP, Van Der Bilt A, et al. Biting and chewing in overdentures, full dentures, and natural dentitions. *J Dent Res.* 2000;79(7):1519–1524. doi:10.1177/00220345000790071501
30. Hattori Y, Satoh C, Kunieda T, Endoh R, Hisamatsu H, Watanabe M. Bite forces and their resultants during forceful intercuspal clenching in humans. *J Biomech.* 2009;42(10):1533–1538. doi:10.1016/j.jbiomech.2009.03.040
31. Quiudini PR Jr, Pozza DH, Pinto ADS, de Arruda MF, Guimarães AS. Differences in bite force between dolichofacial and brachyfacial individuals: Side of mastication, gender, weight and height. *J Prosthodont Res.* 2017;61(3):283–289. doi:10.1016/j.jpor.2016.10.003
32. Quinn JB, Quinn GD. A practical and systematic review of Weibull statistics for reporting strengths of dental materials. *Dent Mater.* 2010;26(2):135–147. doi:10.1016/j.dental.2009.09.006
33. Ritter JE. Critique of test methods for lifetime predictions. *Dent Mater.* 1995;11(2):147–151. doi:10.1016/0109-5641(95)80051-4
34. Silveira MPM, Campaner LM, Bottino MA, Nishioka RS, Borges ALS, Tribst JPM. Influence of the dental implant number and load direction on stress distribution in a 3-unit implant-supported fixed dental prosthesis. *Dent Med Probl.* 2021;58(1):69–74. doi:10.17219/dmp/130847
35. Yang Y, Liu Y, Yuan X, et al. Three-dimensional finite element analysis of stress distribution on short implants with different bone conditions and osseointegration rates. *BMC Oral Health.* 2023;23(1):220. doi:10.1186/s12903-023-02945-9
36. Reda R, Zanza A, Galli M, De Biase A, Testarelli L, Di Nardo D. Applications and clinical behavior of BioHPP in prosthetic dentistry: A short review. *J Compos Sci.* 2022;6(3):90. doi:10.3390/jcs6030090